

Article

Promote Alumina Leaching through Re-Pelleting: Effects of Directional Coating of Calcite on Silicate Grains

Wentao Hu ¹, Qun Qiu ¹, Xinlei Wei ¹, Hong Wei ¹, Qin Zhao ¹, Feihua Yang ² and Xinwei Liu ^{3,*}

¹ State Key Laboratory of High-Efficient Mining and Safety of Metal Mines (USTB), Ministry of Education, Beijing Key Laboratory of Resource-Oriented Treatment of Industrial Pollutants, University of Science and Technology Beijing, Beijing 100083, China; huwentao010@gmail.com (W.H.); s20160105@xs.ustb.edu.cn (Q.Q.); 41501660@xs.ustb.edu.cn (X.W.); 41501646@ustb.edu.cn (Q.Z.)

² State Key Laboratory of Solid Waste Reuse for Building Materials, Beijing Building Materials Academy of Science Research, Beijing 100041, China; chyangfeihua@126.com

³ Industrial Research Department, China Nonferrous Metals Industry Association Recycling Metal Branch, Beijing 100037, China

* Correspondence: liuxw@chinacmra.org; Tel.: +86-010-5889-2436

Received: 22 February 2018; Accepted: 21 March 2018; Published: 23 March 2018



Abstract: The contents of Fe and SiO₂ in ferric bauxite are much higher than that in regular bauxite, and the leaching yield of Al₂O₃ from ferric bauxite cannot reach the general level of ordinary ores, even under optimal conditions. This paper introduces a pretreatment method to enhance sintering before leaching. First, mixing followed by grinding was found to be more efficient than grinding followed by mixing as a pretreatment method by forming a directional coating structure of CaCO₃ on the SiO₂ surface. Second, leaching yields increased grinding fineness because CaCO₃ grain uniformity could be improved with the latter method. Finally, the leaching yields were increased by pulp consistency under certain conditions, as evidenced by improvements in CaCO₃ uniformity, bulk density, and Al₂O₃ grain size, which parameters were beneficial to enhance leaching. The leaching yield of Al₂O₃ was increased from 75.2% to 87.15% by using the proposed mixing–grinding method with the leaching agent of water.

Keywords: leaching; ferric bauxite; pelleting; high-iron bauxite; direct reduction

1. Introduction

Ferric bauxite is highly valuable refractory bauxite that is widely distributed in China, Laos, and Tanzania [1–3], but is improperly used. Numerous creative attempts have been performed for its utilization due to arduous explorations of predecessors. The first attempt is beneficiation. Many researchers engage in separating Fe and SiO₂ from alumina because ferric bauxite contents in the two components were much higher than that in regular ores. Kahn et al. [4] found that separation via gravity was better than that through magnetic force, and the Fe₂O₃ content in the concentrate obtained with the former was only 6%. Solymár et al. [5] investigated separation from microstructure and found that the disadvantages of ferric bauxite are majorly determined by the disseminated particle dimensions and embedded features of minerals. However, complicated textures and structures prevent minerals in ferric bauxite from achieving monomeric separation [6], thereby limiting the industrial application.

Leaching was also popular for disposing of ferric bauxite [7,8]. Papassiopi et al. [9] developed a method involving microbial dissolution, by which the dissolution ratio of Fe from amorphous Fe₂O₃ reached up to 95%; however, only 9% Fe could be leached out in crystal form. Li et al. [8] proposed

an amazing method to convert hematite into magnetite for removing iron. Results showed that most hematite was converted to magnetite by reacting with HFeO_2^- in an alkaline sodium aluminate solution. Quantitative iron powder was added to the solution to regenerate HFeO_2^- so that magnetite could be sequentially produced. However, the authors offered no explanation of the conversion ratio or benefits of the obtained magnetite. Hence, evaluating the commercial value of the leaching manner is still difficult for engineers.

Direct reduction was also introduced for the production of high-grade iron powder [10]. Li et al. [11] reported a gas-based reducing process of ferric bauxite, in which granular iron and carbon black grain with diameters of 0.05–0.2 μm and 0.3–0.1 μm were prepared through reduction at 900 °C. Li et al. [12] optimized the approach by adding a magnetic separation procedure after direct reduction. Results showed that >89% of iron became recyclable metal, whereas 86.09% of aluminum was left in non-magnetic part as alumina concentrate after reduction at 1400 °C and magnetic separation with an intensity of 40 KA/m. Unfortunately, some disadvantages of direct reduction were observed during these explorations; that is, Fe_2O_3 tended to generate to hercynite during the heating progress. This became a limitation for iron and alumina recoveries [12]; hence, a simple direct reduction process failed to achieve commercial utilization. A direct reduction-leaching approach appeared in this academic background [13–15]. It connects direct reduction and leaching processes together, which may convert diasporite and boehmite into water-soluble aluminate by reacting with added sodium carbonate while reducing hematite and goethite into elemental iron and then recycling them through magnetic separation from leach residue. Further information on this new manner was discussed in our previous reports [16–21]. Some defects in this method were also observed, such as the excessive demand of Na_2CO_3 [18,19]. The optimal Al_2O_3 leaching yield was 75.02%, even when the dosage of Na_2CO_3 reached up to 85% [19]. This finding was mostly attributed to the limitation from excess SiO_2 in ferric bauxite. Avoiding extensive Na_2CO_3 consumption is desired by researchers and industries who are concerned with low-grade resources. Tripathi et al. [22] found that the occurrence of sintered grains was related to their chemical compositions. Le et al. [23] proposed a heat transfer mechanism by testing microstructures which involves preheating by vapors and decreasing the penetration depth of the outer layer. However, the influencing factors of forming and property differences between microstructures have not yet been revealed, even though both the final products and heating process were proven to be affected by microstructures. In the current investigation, a directional coated structure—which benefits sintering—was discovered after pregrinding and re-pelleting. The leaching properties of clinker obtained with ferric bauxite and soda lime might be improved by forming the structure. The results obtained may provide a new research foundation on ferric bauxite utilization, and reduce Na_2CO_3 consumption in ordinary bauxite disposal processes by promoting the conversion rate of SiO_2 into a stable form to avoid forming $\text{Na}_2\text{O}\cdot\text{Al}_2\text{O}_3\cdot\text{SiO}_2$, which leads to Al_2O_3 and Na_2O loss.

2. Experimental

2.1. Experimental Materials

The ore used was supplied from the Southwest of China. The chemical composition and XRD pattern of the ore are shown in Table 1 and Figure 1, respectively.

Table 1. Chemical composition of the ore. LOI: loss on ignition.

Composition	Fe_2O_3	Al_2O_3	SiO_2	TiO_2	MgO	CaO	Na_2O	K_2O	P_2O_5	LOI
Contents/% (w/w)	41.13	33.02	12.22	1.49	0.68	0.63	0.32	0.06	0.04	8.97

Table 1 indicates that iron and aluminum are two major recyclable elements in the ferric bauxite. In the table, LOI is the abbreviation form of “loss on ignition”, which was conducted according to GB6730.1-1986, a national standard of China. Hematite and goethite are major iron-bearing minerals, while boehmite and diasporite are found as major aluminum-bearing phases (Figure 1).

However, excess SiO_2 is also noticed in the ferric bauxite adopted (Table 1), and these SiO_2 mainly occurred as Kaolinite (Figure 1). The alumina–silica ratio (A/S) of the sample is only 2.7, which is much lower than those of merchantable ores.

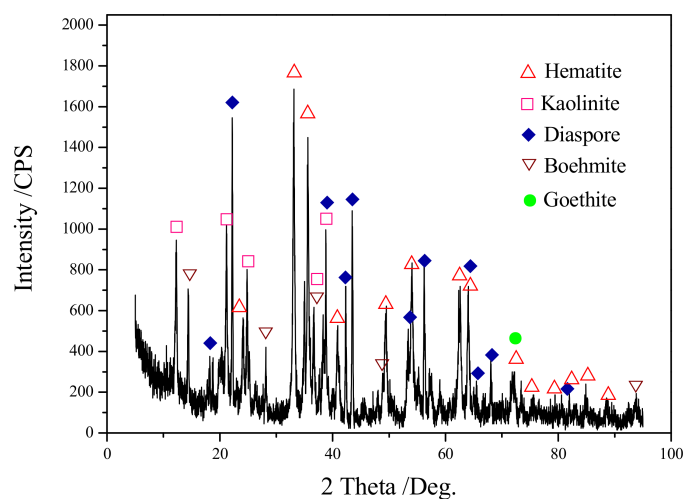


Figure 1. XRD pattern of the ore.

The coal adopted was also supplied from southwest of China. The proximate analysis and the ash chemical compositions of the coal are shown in Tables 2 and 3, respectively.

Table 2. Proximate analysis of the coal used.

Component	Total Moisture (M_t)	Volatiles (V_{ad})	Ash (A_{ad})/%	Fixed Carbon (FC_{ad})
Contents/% (w/w)	9.16	39.42%	5.07%	46.35%

Table 3. Ash chemical compositions of the coal.

Component.	SiO_2	Al_2O_3	Fe_2O_3	MgO	CaO	Na_2O	K_2O	TiO_2	P_2O_5
Contents/% (w/w)	38.0	21.37	36.19	1.9	7.15	0.43	1.38	0.84	0.41

The sodium carbonate and calcium carbonate adopted were analytic reagent (AR) grade and supplied from Guoyao chemical reagent co. LTD, Beijing, China.

2.2. Experimental Instruments

The experimental equipment used included rod mills (Hengcheng, XMB-70, Hangzhou, China), a box furnace (INCH, SX₂-10-13, Beijing, China), an electronic balance (Mettler, AR1140, Zurich, Switzerland), a filter (Hengcheng, XTLZ, Hangzhou, China), an ultrasonicator (Ruibo, BRC-20A, China), and a drying oven (Shuangxu, PH050, Shanghai, China).

The chemical composition of the samples was analyzed using an atomic absorption spectrophotometer (Rayleigh, UV-9600, Beijing, China). The mineral composition of the ore was determined by XRD analysis (Rigaku, TTRIII, Tokyo, Japan). The morphology and microzone chemical compositions of the sample were examined using an electron microscope (ZEISS, EVO 18, Oberkochen, Germany) equipped with an energy-dispersive spectrometer.

2.3. Experimental Methods

Ferric bauxite, Na_2CO_3 , CaCO_3 , and coal were crushed to 100% passing through 2 mm sieve. The dosages of coal, Na_2CO_3 , and CaCO_3 to ore were 30%, 65%, and 15%, respectively, relative to the

ore mass. The materials were pre-ground with 10% water by mass and then dried. Afterwards, 41 g of the pellets obtained was separated into a 100 mL lidded graphite crucible after drying. The crucible was then placed in an electric box furnace at 1150 °C for 35 min in an uncontrolled gaseous atmosphere. The pellet was coated using gold spraying after cooling to prepare the samples to be tested using scanning electron microscopy (SEM) and energy dispersive X-ray analysis (EDS). The other pellets were fine-ground to 95% by passing through a 0.074 mm sieve at a pregrinding concentration (solid concentration) of 50%, and then ultrasonic leached at a water–solid ratio of 15:1, leaching temperature of 90 °C, leaching time of 30 min, ultrasonic power of 0.3 W/cm², and ultrasonic frequency of 20 kHz. The lixivium was filtered, and its volume was recorded.

The leaching yield Al₂O₃, SiO₂, or Na₂O was then calculated from Equation (1):

$$\eta = \frac{c \cdot V_{ol}}{M \cdot \omega}; \quad (1)$$

η , the leaching yield of Al₂O₃, SiO₂, or Na₂O, %;

c , the concentration of Al₂O₃, SiO₂, or Na₂O in lixivium, g/L;

V_{ol} , the initial addition of water for leaching, L;

M , the mass of the mixture before pregrinding, g;

ω , the mass fraction of Al₂O₃, SiO₂, or Na₂O in the mixture before pregrinding, %.

The schematic of the experimental process conducted is shown in Figure 2.

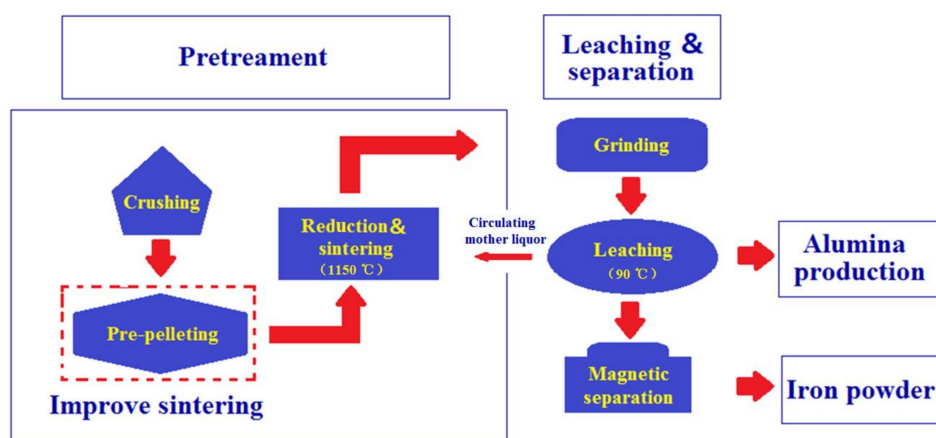


Figure 2. The schematic of the experimental process.

3. Results and Discussion

3.1. Methods of Re-Pelleting

The Fe and Al₂O₃ content of the ferric bauxite failed to achieve the general level of that in ordinary ores, thus reaction efficiencies related to the two components was limited. This is attributed to the many species of minerals distributed in the grains, and the consequent enlarging of spatial distance between grains that prevented Al₂O₃ and Na₂CO₃ from connecting with each other. Two re-pelleting manners—namely, mixing→grinding, and grinding→mixing—were conducted in this research. Mixing→grinding means mixing first followed by grinding, and vice versa.

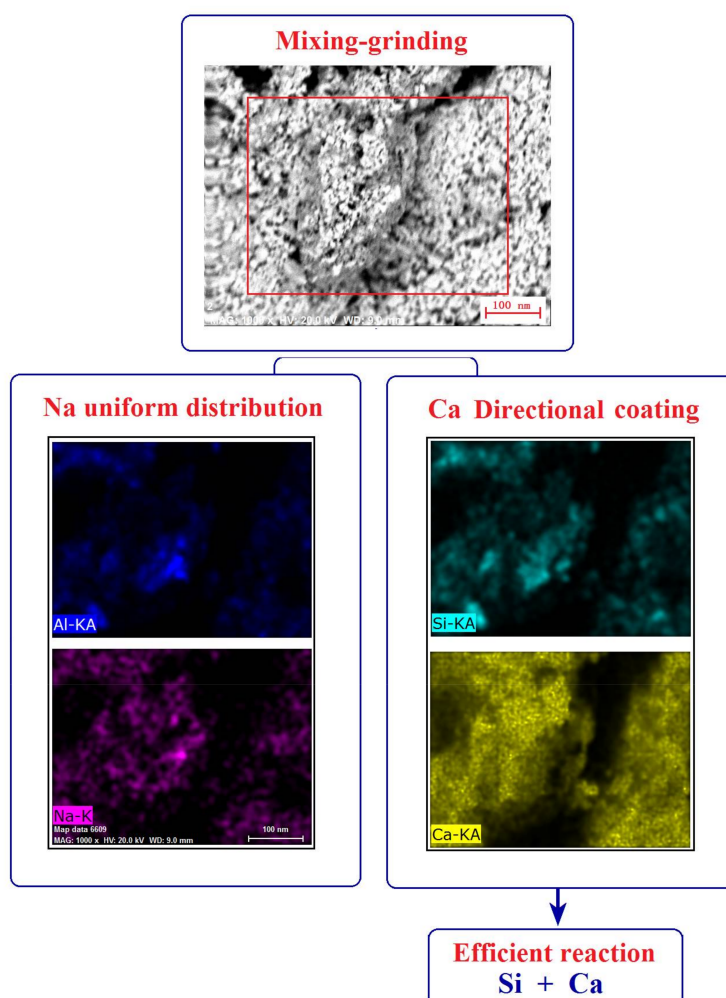
Under the pulp consistency of 60% and pregrinding fineness of 80% passing through −0.038 mm, the leaching yields of the Al₂O₃, SiO₂, and Na₂O of sintered pellet obtained from mixing→grinding and grinding→mixing are shown in Table 4.

Table 4. The leaching yields obtained from two pregrinding manners.

Component	Al ₂ O ₃	SiO ₂	Na ₂ O
Mixing-grinding/% (w/w)	86.78	3.21	72.13
Grinding-mixing/% (w/w)	79.88	9.72	65.54

In the leaching process, Al₂O₃ and Na₂O are expected to be leached out for recycle, while SiO₂ is expected to be left in the residue to increase the lixivium grade. Table 4 shows that the leaching yields of the Al₂O₃ and Na₂O obtained from the pellets after mixing→grinding were higher than that obtained after grinding→mixing; meanwhile, the leaching yield of SiO₂ was lower. This implies that mixing→grinding was better than grinding→mixing as a pretreatment method for improving leaching. The difference in leaching properties of the pellets obtained using the two methods can only be attributed to the directional coating structures, given that the pellets were prepared using materials with the same chemical compositions. At the optimal conditions, the leaching yield of Al₂O₃ obtained after mixing-grinding and sintering reached 86.78%, which was 10.86 percentage points higher than our previous level [19]. Compared to previous experimental methods, only some pre-pelleting procedures were added to the current investigation, while every condition beyond that was kept unchanged.

The elemental maps of sintered pellets obtained after mixing→grinding and grinding→mixing are shown in Figures 3 and 4, respectively.

**Figure 3.** Elemental maps of pellets obtained after mixing→grinding.

As shown in Figure 3, Ca (CaCO_3) was generally found to coat on the surface of Si (SiO_2) grains. However, no similar coating structure was found in Figure 4. This showed that the spatial distance between CaCO_3 on SiO_2 was shortened by forming the directional coating structure; therefore, the reaction efficiency of the two components might be promoted though improving contact probabilities. The mechanism of this promotion can be described as Figure 5.

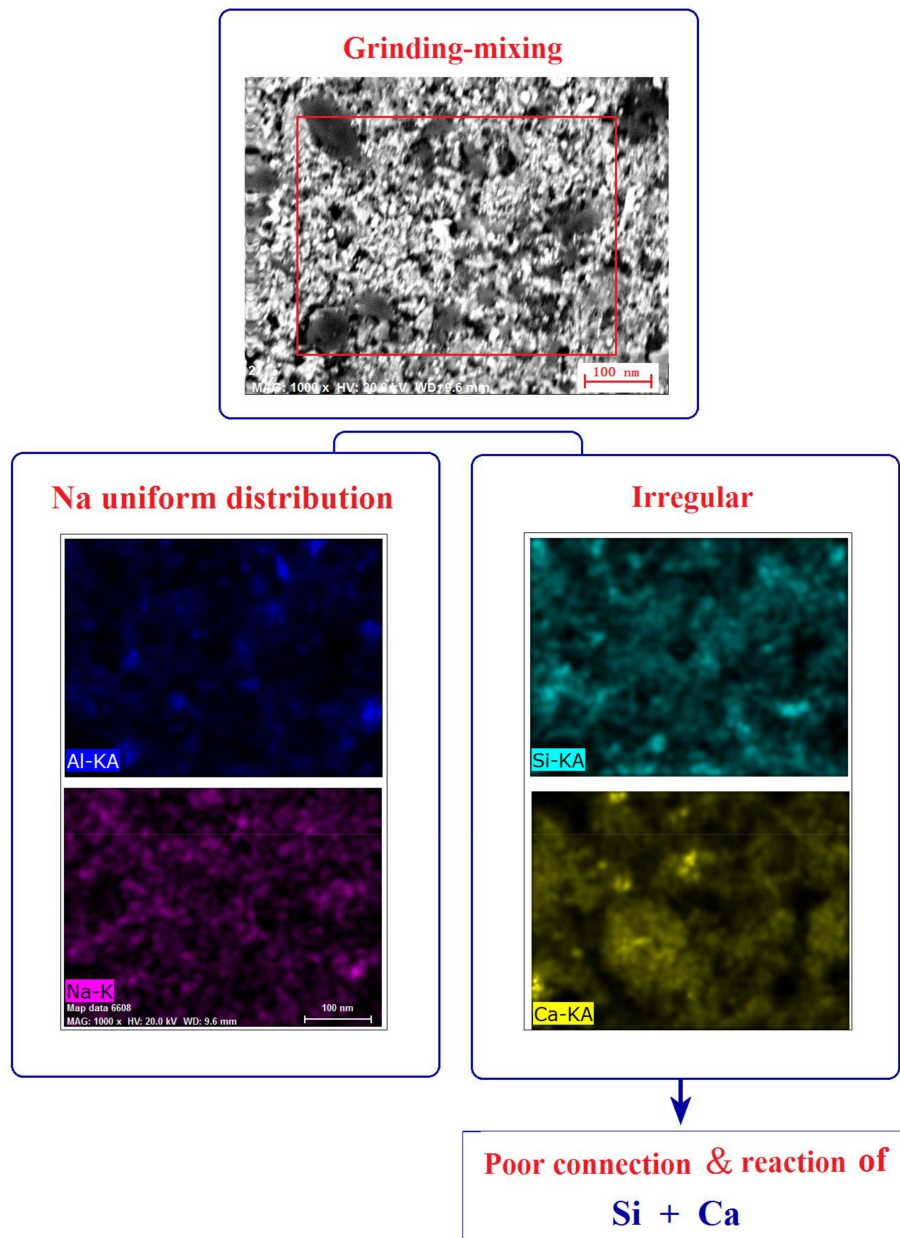


Figure 4. Elemental maps of pellets obtained after grinding→mixing.

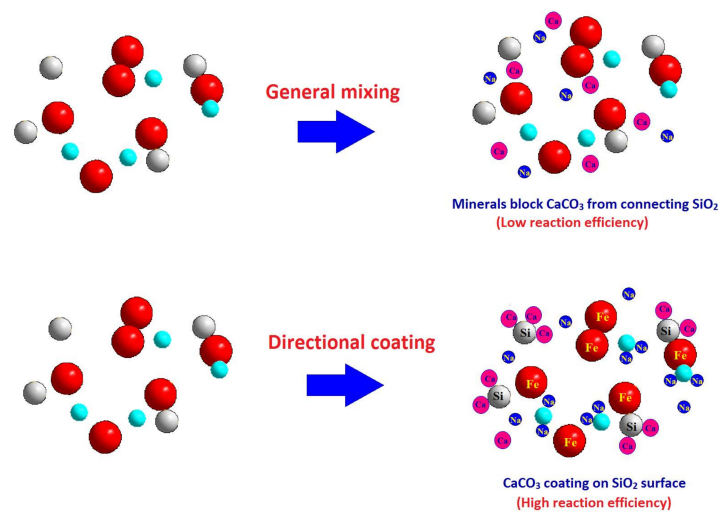


Figure 5. The mechanism of leaching property improvement.

3.2. Pregrinding Fineness

The effects of pregrinding fineness on Al_2O_3 , SiO_2 , and Na_2O leaching yields, and the elemental maps of sintered pellet obtained after mixing \rightarrow grinding with pulp consistency of 60% are shown in Figures 6 and 7, respectively.

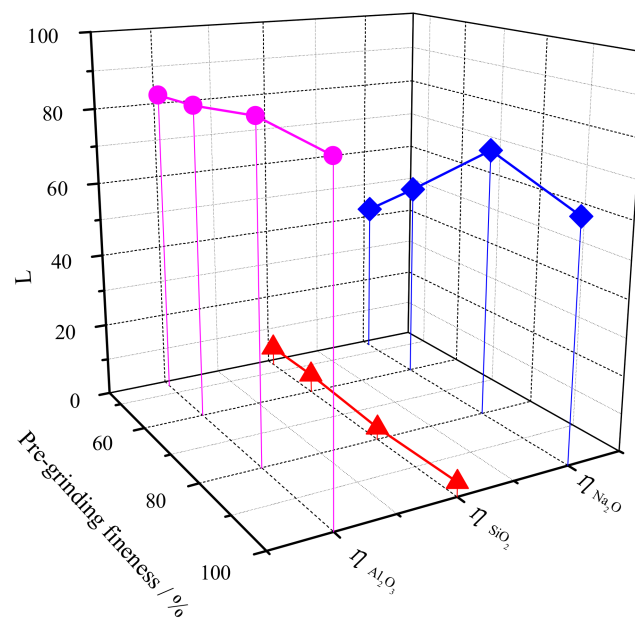


Figure 6. The effects of pregrinding fineness on Al_2O_3 , SiO_2 , and Na_2O leaching yields.

In Figure 6, 46.82% was the fineness of the mixture without pregrinding. The leaching yield of Al_2O_3 and Na_2O was found to reach their maximums, while SiO_2 was found to reach its minimum at the grinding fineness of -0.038 mm 80%. The leaching yield of Al_2O_3 could reach 86.78% by optimizing pulp consistency.

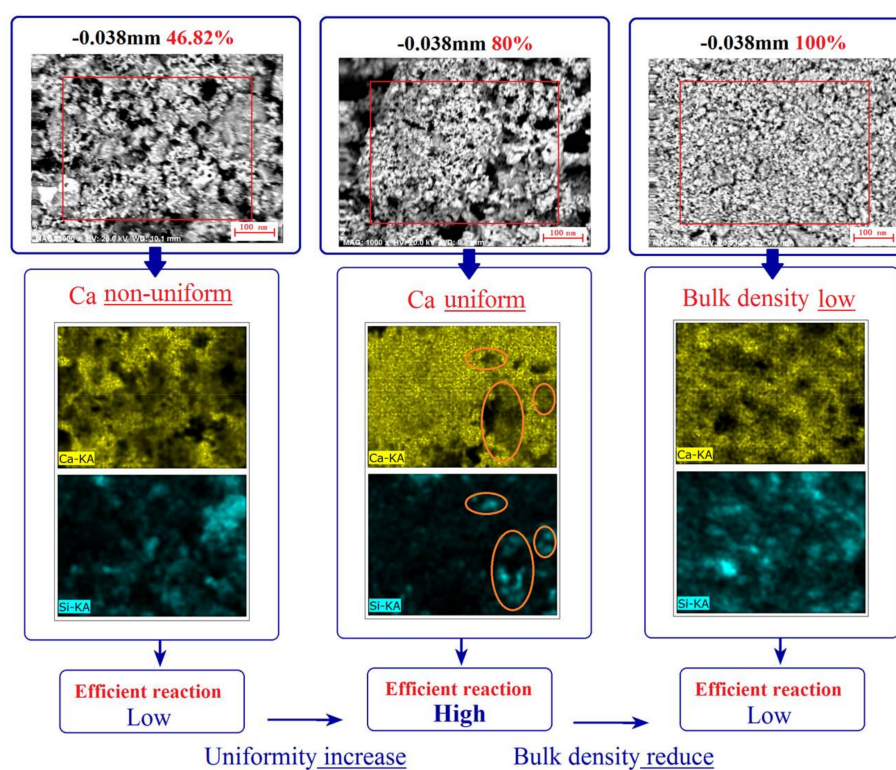


Figure 7. Elemental maps of pellets obtained by adopting grinding fineness of -0.038 mm 46.82%, 80%, and 100%.

A significant difference in leaching yields was observed at the grinding fineness of -0.038 mm 46.82% and 80%, according to Figure 6. However, nothing different in Na distributions was found in Figure 7, implying that the improvement in leaching yields did not come from Na distribution. At the same time, CaCO_3 in the pellet that was found at the grinding fineness of -0.038 mm 80% distributed much more uniformly than that at 46.82%, which might have made the reaction between CaCO_3 and SiO_2 become more efficient [24,25]. Furthermore, the bulk density of pellets obtained at the grinding fineness of -0.038 mm 80% was found to be much denser than that at other grinding fineness. It believed that forming dense pellets was also conducive to shortening the distance between CaCO_3 and SiO_2 grains. Thus, less insoluble $\text{Na}_2\text{O}\cdot\text{Al}_2\text{O}_3\cdot\text{SiO}_2$ was generated and more Na_2O was leached out [25]. On the other hand, once the grinding fineness got close to 100%, most mineral grains in the pellet occurred as fine powders instead of granules, according to Figure 7. Both the bulk density and the spatial distance between the reactant grains failed to reach optimal level. These results explained why the leaching yields obtained from high-grinding-fineness granules decreased with grinding fineness. In short, pregrinding fineness had little effect on directional coating; however, it had a great effect on increasing bulk density, which was also conducive to enhancing leaching.

3.3. Pulp Consistence of Pregrinding

The effect of pregrinding pulp consistency on the leaching yields at grinding fineness of -0.038 mm 80% are shown in Figure 8.

The elemental maps of sintered pellet obtained after mixing-grinding at grinding fineness of -0.038 mm 80% are shown in Figure 9.

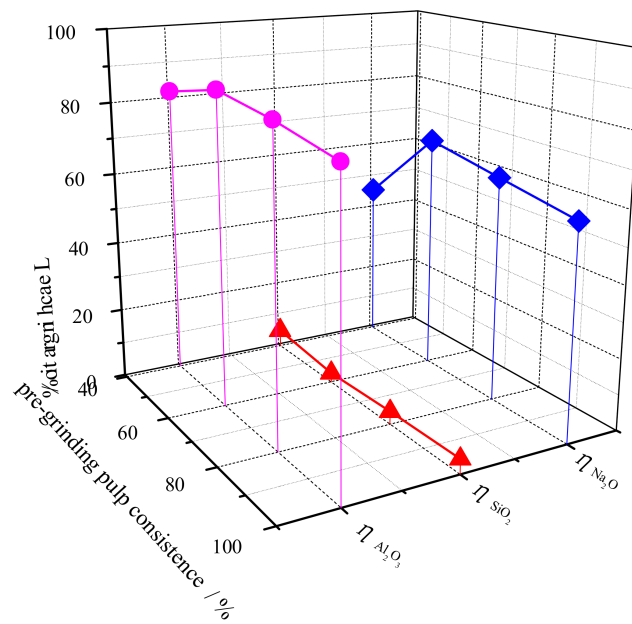


Figure 8. The effect of pregrinding pulp consistency on the leaching yields.

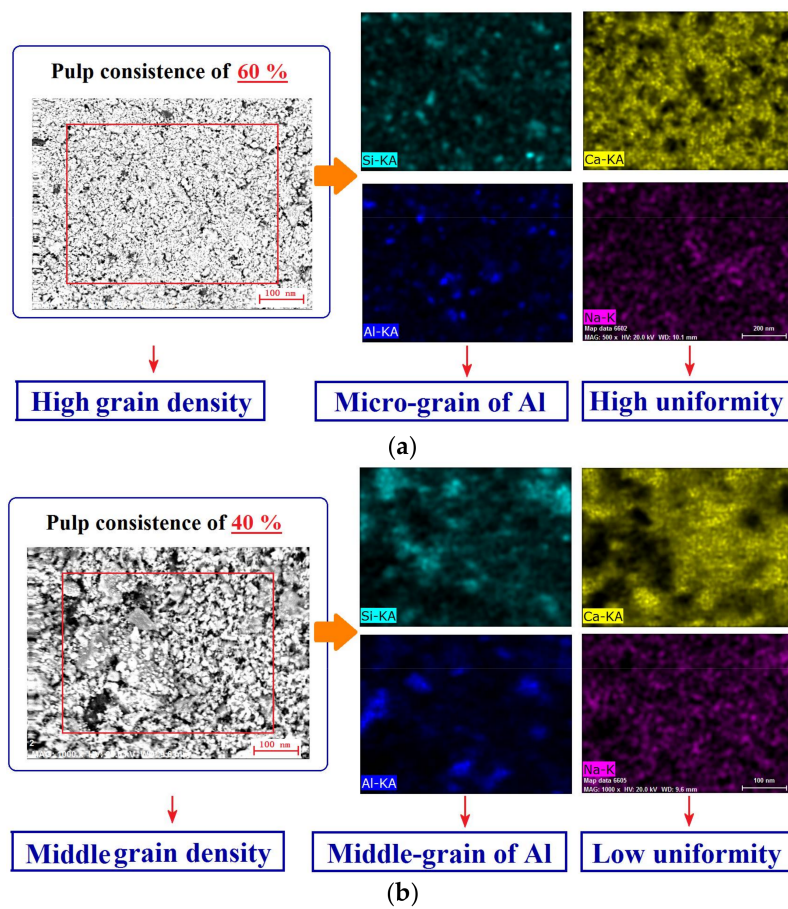


Figure 9. Elemental maps of pellets obtained with the pulp consistency of 40%, 60%, and 100%.

In Figure 8, a pregrinding pulp consistency of 100% means dry grinding. The leaching yields of Al_2O_3 and Na_2O reached their maximums, while SiO_2 reached its minimum at the consistency of -0.038 mm 60%. The reasons for this phenomenon are revealed in Figure 9. The distance between Al_2O_3 and Na_2O grains shortened with the increase of bulk density and the reduction of Al_2O_3 grain size. Thus, the efficiency of the reaction between the Al_2O_3 and Na_2O grains was promoted. The leaching of SiO_2 was also restricted at a pulp consistency of 60% (see Figure 8) because the distribution of CaCO_3 became more uniform at this point (see Figure 9). By optimizing pulp consistency, the leaching yield of Al_2O_3 reached 87.15%.

The silicates consisted of Al_2O_3 and SiO_2 , thus the leaching yields can be improved by avoiding Na_2O , SiO_2 , and Al_2O_3 combining with insoluble nepheline by the fixing the SiO_2 into $2\text{CaO}\cdot\text{SiO}_2$ [26]. However, when the consistency increased from 60% to 100%, all the parameters above mentioned were worsened because of the reduction of grinding efficiencies, as shown in Figure 9. This is because the efficiency of dry grinding (pulp consistency of 100%) was not as high as that of wet grinding, which agreed with the general assumption.

4. Conclusions

(1) Mixing \rightarrow grinding was more efficient than grinding \rightarrow mixing in promoting leaching yields. The directional coating of CaCO_3 on SiO_2 surface increased the reaction efficiency between the two minerals by reducing grain intervals.

(2) The leaching yields Al_2O_3 and Na_2O were promoted by improving CaCO_3 uniformity though increasing pregrinding fineness.

(3) Pulp consistency was a significant affecting factor of CaCO_3 uniformity, bulk density, and Al_2O_3 grain size. The improvement of the latter parameters was beneficial to enhance leaching.

(4) At the optimal conditions, the leaching yield of Al_2O_3 reached 87.15% by the proposed approach. The lixivium obtained can be used for alumina carbonation decomposition and then roasting in order to produce alumina.

Acknowledgments: The authors gratefully acknowledge the support of the State Key Laboratory of Solid Waste Reuse for Building Materials by a grant number SWR-2015-003, the Found of State Key Laboratory of Mineral Processing by a grant number BGRIMM-KJSKL-2015-08, the Fundamental Research Funds for the Central Universities by a grant number FRF-GF-17-B34 and FRF-BR-16-026A, and the National Natural Science Foundation of China by a grant number 51504014.

Author Contributions: Wentao Hu conceived the experiments; Xinwei Liu contributions to the conception; Qun Qiu, Qin Zhao, Xinlei Wei, and Hong Wei performed the experiments; Wentao Hu contributed experimental materials and analysis tools; Wentao Hu wrote the paper; Feihua Yang and Xinwei Liu made the final modification.

Conflicts of Interest: The authors declare no conflicts of interest.

References

1. Deng, J.; Wang, Q.F.; Yang, S.J.; Liu, X.F.; Zhang, Q.Z.; Yang, L.Q.; Yang, Y.H. Genetic relationship between the Emeishan plume and the bauxite deposits in Western Guangxi, China: Constraints from U–Pb and Lu–Hf isotopes of the detrital zircons in bauxite ores. *J. Asian Earth Sci.* **2010**, *37*, 412–424. [[CrossRef](#)]
2. Zhang, Z.W.; Zhou, L.J.; Li, Y.J.; Wu, C.Q.; Zheng, C.F. The “coal-bauxite-iron” structure in the ore-bearing rock series as a prospecting indicator for southeastern Guizhou bauxite mines. *Ore Geol. Rev.* **2013**, *53*, 145–158. [[CrossRef](#)]
3. Cheng, G.; Gao, G.M.; Chen, S.L. Geological characteristics and mineralization regularity of bauxite in Boloven Plateau Laos. *J. Cent. South Univ. (Sci. Technol.)* **2008**, *39*, 380–386.
4. Kahn, H.; Ml, M.; Tassinari, G.; Ratti, G. Characterization of bauxite fines aiming to minimize their iron content. *Miner. Eng.* **2003**, *16*, 1313–1315. [[CrossRef](#)]
5. Solymár, K.; Má dai, F.; Papanastassiou, D. Effect of bauxite microstructure on beneficiation and processing. In *Essential Readings in Light Metals*; Springer: Berlin, Germany, 2016; Volume 1, pp. 37–42.
6. Thair, A.A. Mineralogy, geochemistry, and ore formation of Nuwaifa bauxite deposit, western desert of Iraq. *Arab J. Geosci.* **2017**, *10*, 1–15.

7. Peng, Z.; Hwang, J.Y. Microwave-assisted metallurgy. *Int. Mater. Rev.* **2015**, *60*, 30–63. [[CrossRef](#)]
8. Li, G.H.; Gu, F.Q.; Luo, J.; Deng, B.N.; Peng, Z.W.; Jiang, T. Recovery of iron-titanium-bearing constituents from bauxite ore residue via magnetic separation followed by sulfuric acid leaching. In *Light Metals*; Springer: Berlin, Germany, 2017; pp. 75–81.
9. Papassiopi, N.; Vaxevanidou, K.; Paspaliaris, I. Effectiveness of iron reducing bacteria for the removal of iron from bauxite ores. *Miner. Eng.* **2010**, *23*, 25–31. [[CrossRef](#)]
10. Liu, Z.G.; Chu, M.S.; Wang, Z.; Zhao, W.; Tang, J. Study on metallized reduction and magnetic Separation of iron from fine particles of high iron bauxite ore. *High Temp. Mater. Process.* **2016**, *36*, 1–8. [[CrossRef](#)]
11. Li, Z.; Jin, J.; Wang, Y.; Wu, Y. Study on preparation of iron powder and nano-carbon black by reaction process of high-iron bauxite and natural gas. *Integr. Ferroelectr.* **2015**, *160*, 160–168. [[CrossRef](#)]
12. Li, G.H.; Luo, J.; Jiang, T.; Li, Z.X.; Peng, Z.W.; Zhang, Y.B. Digestion of Alumina from Non-Magnetic Material Obtained from Magnetic Separation of Reduced Iron-Rich Diasporic Bauxite with Sodium Salts. *Metals* **2016**, *6*, 294. [[CrossRef](#)]
13. Hu, W.T.; Wang, H.J.; Liu, X.W.; Sun, C.Y. Effect of nonmetallic additives on iron grain grindability. *Int. J. Miner. Process.* **2014**, *130*, 108–113. [[CrossRef](#)]
14. Hu, W.T.; Wang, H.J.; Liu, X.W.; Sun, C.Y. Correlation between aggregation structure and tailing mineral crystallinity. *Int. J. Miner. Metall. Mater.* **2014**, *21*, 845–850. [[CrossRef](#)]
15. Yeh, C.H.; Zhang, G.Q. Stepwise carbothermal reduction of bauxite ores. *Int. J. Miner. Process.* **2013**, *124*, 1–7. [[CrossRef](#)]
16. Hu, W.T.; Wang, H.J.; Liu, X.W.; Sun, C.Y.; Duan, X.Q. Restraining sodium volatilization in the ferric bauxite direct reduction system. *Minerals* **2016**, *6*, 31. [[CrossRef](#)]
17. Hu, W.T.; Liu, X.W.; Wang, H.J.; Dai, X.J.; Pan, D.L.; Li, J.; Sun, C.Y.; Xia, H.W.; Wang, B. Improvement of sodium leaching ratio of ferric bauxite sinter after direct reduction. *Minerals* **2017**, *7*, 10. [[CrossRef](#)]
18. Hu, W.T.; Wang, H.J.; Liu, X.W.; Sun, C.Y. Effects of Minerals in Ferric Bauxite on Sodium Carbonate Decomposition and Volatilization. *J. Cent. South Univ.* **2015**, *46*, 2503–2507. [[CrossRef](#)]
19. Hu, W.T.; Wang, H.J.; Sun, C.Y.; Ji, C.L.; He, Y.; Wang, C.L. Alkali consumption mechanism on ferrous bauxite reduction process. *J. Cent. South Univ. (Sci. Technol.)* **2012**, *43*, 1595–1603.
20. Hu, W.T.; Wang, H.J.; Sun, C.Y.; Tong, G.K.; Ji, C.L. Direct reduction-leaching process for high ferric bauxite. *J. Univ. Sci. Technol. Beijing* **2012**, *34*, 506–511.
21. Hu, W.T.; Xia, H.W.; Pan, D.L.; Wei, X.L.; Li, J.; Dai, X.J.; Yang, F.H.; Lu, X.; Wang, H.J. Difference of zinc volatility in diverse carrier minerals: The critical limit of blast furnace dust recycle. *Miner. Eng.* **2018**, *116*, 24–31. [[CrossRef](#)]
22. Tripathi, H.S.; Ghosh, A.; Halder, M.K.; Muktherjee, B.; Maiti, H.S. Microstructure and properties of sintered mullite developed from Indian bauxite. *Bull. Mater. Sci.* **2012**, *35*, 639–643. [[CrossRef](#)]
23. Le, T.; Ju, S.H.; Lu, L.M.; Peng, J.H.; Zhou, L.X.; Wang, S.X. A novel process and its mechanism for recovering alumina from diasporic bauxite. *Hydrometallurgy* **2017**, *169*, 124–134. [[CrossRef](#)]
24. Kłosek-Wawrzyn, E.; Małolepszy, J. The potential use of calcite wastes in the production of clay masonry units. *Mater. Ceram.* **2016**, *68*, 230–235.
25. Mandal, A.K.; Sinha, O.P. Effect of Bottom ash fineness on properties of red mud geopolymer. *J. Solid Waste Technol. Manag.* **2017**, *43*, 26–35. [[CrossRef](#)]
26. Bazhin, V.Y.; Brichkin, V.N.; Sizyakov, V.M.; Cherkasova, M.V. Pyrometallurgical treatment of a nepheline charge using additives of natural and technogenic origin. *Metallurgist* **2017**, *61*, 147–154. [[CrossRef](#)]

